

## Microarray-Based Phospho-Proteomic Profiling of Complex Biological Systems<sup>1,2</sup>

C. Rory Goodwin<sup>\*,†,¶</sup>, Crystal L. Woodard<sup>†</sup>, Xin Zhou<sup>‡,¶</sup>, Jianbo Pan<sup>§</sup>, Alessandro Olivi<sup>\*</sup>, Shuli Xia<sup>¶</sup>, Chetan Bettegowda<sup>\*</sup>, Daniel M. Sciubba<sup>\*</sup>, Jonathan Pevsner<sup>¶</sup>, Heng Zhu<sup>†</sup> and John Laterra<sup>‡,¶</sup>

<sup>\*</sup>Department of Neurosurgery, The Johns Hopkins University School of Medicine, Baltimore, MD, USA;

<sup>†</sup>Department of Pharmacology and Molecular Sciences, The Johns Hopkins University School of Medicine, Baltimore, MD, USA;

<sup>‡</sup>Department of Neurology, The Johns Hopkins University School of Medicine, Baltimore, MD, USA;

<sup>§</sup>Department of Ophthalmology, The Johns Hopkins University School of Medicine, Baltimore, MD, USA;

<sup>¶</sup>Hugo W. Moser Research Institute at Kennedy Krieger, Baltimore, MD, USA

### Abstract

Protein microarray technology has been successfully used for identifying substrates of purified activated kinases. We used protein microarrays to globally interrogate the effects of PTEN and Akt activity on the phospho-kinome of *in vitro* and *in vivo* glioma models and validated results in clinical pathological specimens. Whole cell lysates extracted from tumor samples can be applied to human kinome chip microarrays to profile the global kinase phosphorylation patterns in a high-throughput manner and identify novel substrates inherent to the tumor cell and the interactions with tumor microenvironment. Our findings identify a novel microarray-based method for assessing intracellular signaling events applicable to human oncogenesis and other pathophysiological states.

*Translational Oncology* (2016) 9, 124–129

### Introduction

Many oncogenic mechanisms are regulated through posttranslational protein modifications, which most commonly include phosphorylation, acetylation, methylation, ubiquitination, and SUMOylation [1]. Protein phosphorylation, which is mediated by 525 annotated protein kinases, is estimated to influence up to 30% of the proteome and regulates fundamental cellular processes such as cell proliferation, apoptosis, migration, and angiogenesis [1–3]. Global analyses of these intracellular signaling networks are critical to our understanding of oncogenesis and to the advancement of novel cancer therapeutics.

Knowledge of signaling events that drive malignancy is often limited by experimental analyses that rely on the isolation and assessment of singular variables. Our understanding of oncogenic signaling networks and their contribution to cancer phenotypes requires methodologies that globally analyze protein phosphorylation events in cells and tissues. Protein microarray technology has been validated previously as a tool for identifying candidate substrates of purified kinases [4]. Hyperactivation of receptor tyrosine kinases and their downstream effector pathways is a characteristic of multiple solid

Address all correspondence to: C. Rory Goodwin, MD/PhD, Department of Neurosurgery, The Johns Hopkins University School of Medicine, Hugo W. Moser Research Institute, at Kennedy Krieger, Inc., 707 North Broadway, Baltimore, MD 21205.

E-mail: [rory@jhmi.edu](mailto:rory@jhmi.edu)

<sup>1</sup>This work is supported in part by the National Institutes of Health (RO1 CA129192 and RO1 NS43987 to J.L.) and the United Negro College Fund/Merck Science Initiative, Neurosurgery Research and Education Foundation, and Burroughs Wellcome Fund to C. R. G.

<sup>2</sup>Contribution statement: C. R. G., C. K. W., H. Z., and J. L. contributed to study conception and design. C. R. G., C. L. W., X. Z., A. O., S. X., C. B., and D. M. S. contributed to acquisition of data. C. R. G., S. X., J. P., H. Z., and J.L. contributed to analysis and interpretation of data. C. R. G. and J. L. contributed to drafting of manuscript. All authors contributed to critical revision and final approval of submitted manuscript. Received 20 November 2015; Revised 16 February 2016; Accepted 17 February 2016

© 2016 The Authors. Published by Elsevier Inc. on behalf of Neoplasia Press, Inc. This is an open access article under the CC BY-NC-ND license (<http://creativecommons.org/licenses/by-nc-nd/4.0/>).

1936-5233/16

<http://dx.doi.org/10.1016/j.tranon.2016.02.001>

malignancies and occurs in more than 85% of glioblastoma [5]. Akt, a serine/threonine kinase that is activated through serine-473 phosphorylation, serves as a key node within oncogenic receptor tyrosine kinase signaling networks. Akt hyperactivation commonly results from loss of function of the tumor-suppressing dual-specificity phosphatase PTEN, which is commonly mutated or deleted in solid malignancies including 40% to 50% of glioblastomas. Activating Akt mutations have been found in 22% to 87% of solid malignancies and up to 54% of gliomas [5]. Here we describe the novel application of protein microarray technology to globally assess the influence of PTEN function on the phospho-kinome of glioma cells *in vitro* and glioma xenografts *in vivo*. Specifically, we used a tet-inducible system

to investigate how Akt deactivation, as a downstream consequence of PTEN reconstitution, regulates known and novel protein substrates implicated in glioma malignancy. This global analysis identifies a novel microarray-based method for assessing intracellular signaling events underlying human oncogenesis.

**Results**

We asked if protein microarray technology, similar to that previously developed for the evaluation of substrates of purified kinases, can be used to analyze more complex and biochemically heterogeneous cells and tissues toward the goal of understanding complex cell signaling cascades, such as those associated with oncogenic signal regulation

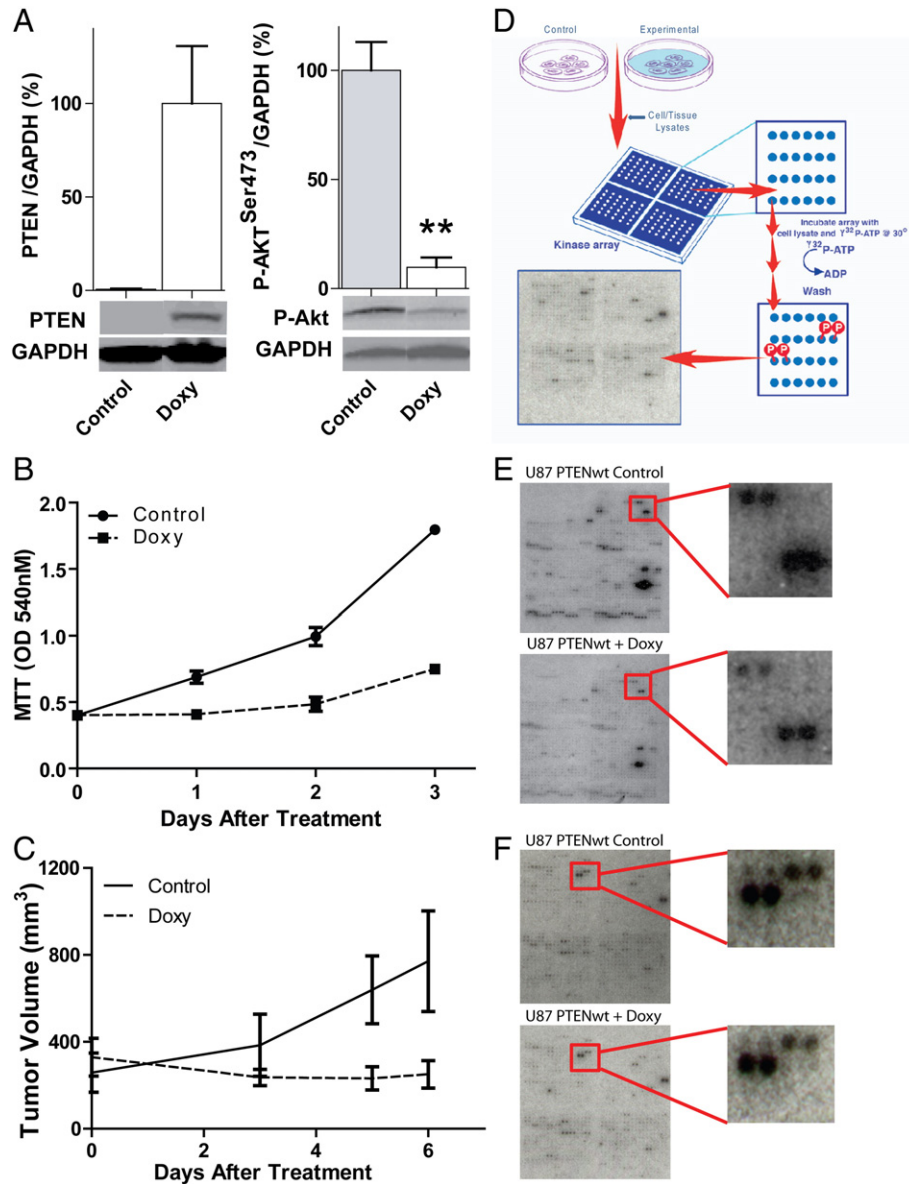


**Figure 1.** (A) Immunoblot analysis of PTEN expression and phospho-Akt levels in U87 glioma cells +/- PTEN-reconstitution (Doxycycline/Doxy). (B) MTT analysis of U87 glioma cell +/- Doxy demonstrates decreased cell growth in U87 cells in response to PTEN induction by Doxy. (C) U87 glioma xenografts +/- Doxy demonstrate decreased tumor growth in response to PTEN induction by Doxy. (D) Experimental paradigm used to evaluate effect of PTEN reconstitution (control versus experimental) on the U87 glioma cell kinome using human protein microarrays. (E) Whole cell lysates from U87 glioma cells +/- Doxy and (F) whole tissue lysates from U87 glioma xenografts +/- Doxy analyzed on human kinase microarrays with magnified representative section demonstrating decreased substrate phosphorylation in response to doxycycline.

(Figure 1A). Conditions for detecting the largest number of phosphorylation events in response to incubating protein microarrays with control whole cell lysates were optimized by varying the concentrations of whole cell lysate protein and time of incubation on the microarrays. HEK93 cell lysates were diluted to achieve final protein concentrations ranging from 0 to 0.8  $\mu\text{g}/\mu\text{l}$  and then incubated on protein microarrays in the presence of  $^{32}\text{P}$ - $\gamma$ -ATP for 0, 10, 30, 60, and 120 minutes as previously described with modifications [3,4] (Supplemental Figure 1). Reactions were terminated by washing microarrays with Tris-buffered saline (TBS) containing 0.1% Tween 20 (TBS/T) and SDS buffers to ensure that the radioactivity detected on the arrays was due to covalent phosphorylation, and phosphorylation signals were then visualized by autoradiography and analyzed using the GenePix

software as described in Materials and Methods. All experiments were carried out using optimized conditions (0.2  $\mu\text{g}/\mu\text{l}$  of lysate concentration and 30-minute incubation time) (Supplemental Figure 2).

Human U87 glioma cells, engineered to express PTEN via a tet-on promoter system (U87-tetPTEN), were used to examine the global effects of PTEN reconstitution on the cell phospho-kinome [6]. We quantified the effects of doxycycline on the induction of PTEN and Akt phosphorylation (Ser473) and the biological response of glioma cell growth *in vitro* and tumor xenograft growth *in vivo*. PTEN was robustly increased, and Akt phosphorylation was inhibited by  $\sim 90\%$  ( $P < .05$ ) after incubating cells with doxycycline for 24 hours (Figure 1B). PTEN reconstitution *in vitro* inhibited cell growth by  $\sim 70\%$  (Figure 1B), and treating animals following cell implantation

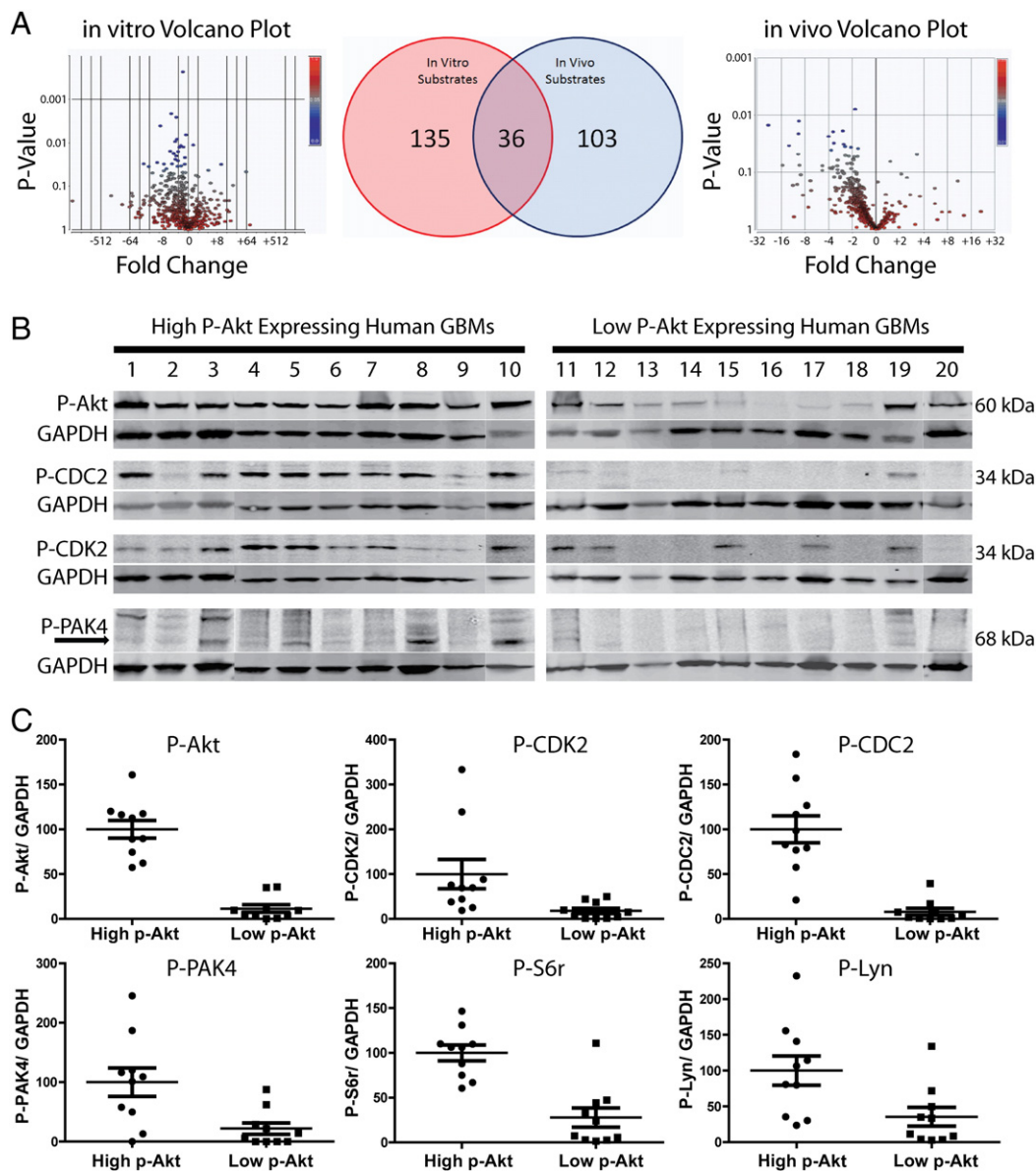


**Figure 2.** Identification and confirmation of PTEN-regulated kinase substrates. (A) Volcano plot analyses of results obtained from cultured glioma cells (*in vitro*; left panel) and glioma xenografts (*in vivo*; right panel) identified substrates organized by fold-change intensity and  $P$  value significance. Venn diagram shows the number of PTEN-regulated phosphorylated substrates identified via the human protein microarray. (B) Immunoblot of 20 primary human GBM samples stratified based on high and low phospho-Akt (Ser473) expression (p-Akt<sup>high</sup> and p-Akt<sup>low</sup>) showing phosphorylated forms of candidate kinase substrates identified by microarray. (C) Scatter plots of relative levels of phospho-CDK2, phospho-CDC2, phospho-PAK4, phospho-s6r, and phospho-Lyn in p-Akt<sup>high</sup> and p-Akt<sup>low</sup> clinical gliomas.

with doxycycline arrested the growth of subcutaneous tumor xenografts, which were ~60% smaller than controls on posttreatment day 6 ( $P < .05$ ) (Figure 1C). These cell and tumor xenograft responses are consistent with PTEN's known signaling and tumor-suppressive biological activities and establish the conditions for using this model to study global effects of PTEN on the glioma cell phospho-kinome.

Whole cell (*in vitro*) or whole tumor (*in vivo*) lysates obtained from control and doxycycline-treated conditions were incubated on human protein microarrays in the presence of  $^{32}\text{P}$ - $\gamma$ -ATP at 30°C, and microarrays were processed essentially as described in Materials and Methods and depicted in Figure 1, D–F. Partek software was used to analyze and compare the number and relative intensity of protein phosphorylation events on the microarrays. Figure 2A (left and right panels) depicts the fold-change by volcano plot for all phosphorylation events from *in vitro* and *in vivo* lysates, and the Venn diagram (middle panel) demonstrates the number of distinct and common *in vitro* and *in vivo* phosphorylation events. PTEN reconstitution *in vitro* decreased the phosphorylation of 36, 103, and 135 protein targets using  $P < .05$ ,  $P < .15$ , and  $P < .20$ , respectively, as statistical cutoffs (Supplementary Table 1). This analysis identified phospho-ribosomal S6 kinase polypeptide and phospho-CDC2, two differentially phosphorylated targets that are known to regulate cell cycle progression at the G2/M checkpoint (see Supplemental Material), as well as the second messenger molecules MAPK and Akt. Immunoblot analyses of control and doxycycline-treated U87-tetPTEN cell lysates confirmed that PTEN induction reduced endogenous phospho-ribosomal S6 kinase polypeptide by ~95% ( $P < .05$ ) and phospho-CDC2 by ~50% ( $P < .05$ ) (Supplementary Figure 3). PTEN induction *in vivo* reduced the phosphorylation of 16, 67, and 103 microarray protein targets at  $P < .05$ ,  $P < .15$ , and  $P < .20$  statistical cutoffs, respectively (Supplementary Table 2). Similar to the *in vitro* results, the *in vivo* analysis identified phospho-ribosomal S6 kinase polypeptide, MAPK, Akt, and phospho-CDK2 (Table 1). Immunoblot analyses of tumor lysates confirmed that PTEN induction inhibited the phosphorylation of endogenous ribosomal S6 kinase by ~65%, CDK2 by ~50%, PAK4 by ~65%, and MAPK by ~55% ( $P < .05$ ), validating the ability of protein microarrays to predict phospho-kinome dynamics *ex vivo* (Supplementary Figure 3).

Akt is one of the most proximal downstream effectors of PTEN reconstitution predicting that the PTEN-regulated phospho-proteins identified by microarray analysis would correlate with the phosphorylation status of AKT in clinical tumor specimens. Twenty clinical WHO grade IV gliomas were obtained and stratified by semiquantitative immunoblot analysis into high phospho-Akt expressers and low phospho-Akt expressers. The 10 clinical specimens that expressed

the highest levels of phospho-Akt using the Odyssey Infrared Imager (LI-COR Biosciences) were placed in the “high phospho-Akt expressers,” and the remaining clinical specimens were placed in the “low phospho-Akt expressers.” We then analyzed tumor lysates by immunoblot for five phospho-proteins shown to be PTEN-regulated (*in vitro* or *in vivo*) by the protein microarray assays described above. The five candidate phospho-proteins were chosen based on their known function as regulators of cell growth and/or cell cycle progression and antibody availability. As predicted by microarray, the low-phospho-Akt glioblastomas had statistically significantly lower phosphorylated forms of these five phospho-proteins than the high-phospho-Akt glioblastomas (Figure 2, B and C). Specifically, phospho-CDK2 was reduced by ~85%, phospho-CDC2 by ~90%, phospho-ribosomal S6 kinase polypeptide by ~70%, phospho-PAK4 by ~80%, and phospho-Lyn by ~70% in low-phospho-Akt specimens. Thus, microarray analysis correctly predicted associations between Akt activity and protein phosphorylation status in clinical specimens.

## Discussion

In conclusion, we show that the human kinase protein microarrays offer an effective high-throughput platform to profile global kinase phosphorylation patterns in lysates obtained from whole cells and tissues. This methodology does not rely on the availability or specificity of antibodies or other types of affinity reagents, which can be problematic. Compared with tandem mass spectrometry approaches, this microarray technique offers cost-effectiveness and exceedingly high throughput for generating an activity-based profile of the human kinome in complex biological systems. The *in vitro* and *in vivo* glioma models used in this study generated overlapping but distinct phospho-protein patterns. These differences can be attributed to any of the many characteristics that differentiate the two model systems including but not limited to tumor microenvironment effects and stromal cells in the more complex tumor xenografts. Traditional immunoblot analysis of clinical glioma specimens for candidate phospho-protein substrates identified in preclinical glioma models by microarray validated the predictive value of the protein microarray method. Human protein microarray technology offers a new high-throughput method for performing unbiased global analyses of intracellular signaling networks underlying malignancy and other pathologic processes.

## Materials and Methods

### Human Open Reading Frame (ORF) Cloning

Using the Gateway recombinant cloning system (Invitrogen, CA), human ORFs were shuttled from the selected entry clones of the Ultimate Human ORF Collection (Invitrogen, CA) to a yeast high-copy expression vector (pEGH-A) that produces 6x-His-GST fusion proteins under the control of the galactose-inducible GAL1 promoter [4]. Plasmids were rescued into *Escherichia coli* and verified by restriction endonuclease digestion. Plasmids with inserts of correct size were transformed into yeast for protein purification (see Supplementary Information).

### Protein Purification and Proteome Arrays

The human kinase proteins were purified as 6x-His-GST fusion proteins from yeast using a high-throughput protein purification protocol similar to that described previously [7]. Human kinome protein microarrays were custom-made slides and subjected to

**Table 1.** Overlapping *In Vitro* and *In Vivo* Substrate List

Column ID		
ADRBK2	His-Avi	PRKACA
AURKC	ILK	PRKACB
C9orf96	LYK5	RPS6KA4
CAMK2A	LYN	SRPK2
CCL2	MAP2K4	SYK
CDC2	MAP3K7	TBK1
CDK2	MAPK11	TRIM27
CDKN1A	MAPK13	TTBK2
CSNK2A1	MAPKAPK5	WIF1
DAPK2	NRP2	XRCC6BP1
DCLK1	PDGFRL	ZAP70
H2B (100ug/ml)	PKB/AKT com	rnlL2a

anti-GST probing to measure the total protein impregnated in each chip using previously established protocols [3,4]. In brief, about 520 yeast strains that consistently overexpress yeast proteins as GST fusions were used to prepare protein chips. GST fusion proteins were bound to glutathione beads (GE Healthcare) for 1 hour at 4°C, washed four times with wash buffer I (50 mM Tris-HCl [pH 7.5], 500 mM NaCl, 1 mM EGTA, 10% glycerol, 0.1% Triton X-100, 0.1% β-mercaptoethanol, and 0.5 mM PMSF) and two times with wash buffer II (50 mM HEPES [pH 7.4], 100 mM NaCl, 1 mM EGTA, 10% glycerol, 0.1% β-mercaptoethanol, and 0.5 mM PMSF), and eluted in elution buffer (50 mM HEPES [pH 7.4], 100 mM NaCl, 40 mM reduced glutathione, 0.03% Triton X-100, and 30% glycerol). Each kinase protein was assayed by *in vitro* dot blot by incubating at 30°C for 30 minutes in the presence of kinase buffer, and the reaction was terminated by heating the mixture at 90°C for 5 minutes. The majority of the proteins were not able to autophosphorylate under these conditions. Protein products that were successfully purified based on immunoblot analysis were then spotted in duplicate onto surface-modified glass (Full Moon Biosystems) microscope slides using a 48-pin contact printer (Bio-Rad).

### Elimination of Printing Bias

Multiple array comparisons were critical for optimizing the dynamic kinase assays performed on the protein microarrays. To ensure the equality of the arrays used to perform the dynamic kinase assays, the signal intensities of each protein coordinate were required to be greater than the threshold on all anti-GST arrays. Taking into consideration the signal intensity of each protein coordinate imprinted on the anti-GST X scan of each microarray, only proteins on the anti-GST microarrays with  $Z$  score  $>3$  were used for further analyses. Positive and negative control proteins (i.e., BSA and histones) were excluded from the analyses.

### Phosphorylation Assay and Data acquisition

Cell lysate samples were assayed to determine the protein concentration needed to achieve optimal signal:noise ratio using test protein chips (see Supplementary Information). Proteome arrays were blocked in  $1 \times$  TBST containing 0.1% BSA (Roche) for 30 minutes at 30°C with gentle shaking. Lysates were diluted into kinase buffer (50 mM Tris-HCl [pH 7.5], 100 mM NaCl, 10 mM, MgCl<sub>2</sub>, 1 mM MnCl<sub>2</sub>, 1 mM DTT, 1 mM EGTA, 25 mM Hepes-KOH [pH 7.5], 2 mM NaVO<sub>4</sub>, 2 mM NaF, 0.01% cold ATP, and γ-32P-ATP [33.3 nM final concentration]) and incubated on cover-slipped arrays in a humidified chamber at 30°C for 30 minutes in triplicate (see Lysate Methods in Supplemental Information). The arrays were subjected to three 10-minute washes in  $1 \times$  TBST (pH 7.5), three 10-minute washes in 0.5% SDS, and one quick rinse with distilled water before spin drying and X-ray film (Kodak) exposure. Control arrays were incubated with kinase reaction mixture without protein lysate and processed in parallel. Three sets of exposures were taken for each kinase assayed: 10, 17, and 24 hours. The X-ray film was scanned at 4800 dots per inch and analyzed using Genepix 3.0 (Molecular Devices). The optimal exposure was selected for each set of experiments and compared with the corresponding control slides.

### Identification of Positive Hits

For the microarray analysis of both *in vitro* cell models and *in vivo* xenografts, a  $\Delta Z$  score (representing the  $Z$ -score difference between treatment and control experimental arrays) was calculated for each

protein represented on the microarray. For the selected  $\Delta Z$  cutoff,  $Z_0$ , we obtained a number of differentially phosphorylated proteins,  $H(Z_0)$ , and calculated corresponding  $P$  values. To determine an optimal cutoff, we calculated an enrichment score using

$$E_n = \frac{\frac{H(Z_0)}{P(Z_0)}}{n_P}$$

where  $P(Z_0)$  is number of all differentially phosphorylated proteins under the cutoff  $Z_0$ , and  $n_H$  and  $n_P$  are total numbers of proteins and all proteins on the chip, respectively. The final  $\Delta Z$  cutoffs were then optimized by the maximum enrichment score recovered.

### Background Correction and Normalization of Protein Microarrays

The raw signal intensity of each array coordinate corresponding to immobilized protein was defined as the foreground median intensity divided by its local background median intensity as acquired using the GenePix software. More than 1000 “empty” or “blank” coordinates on each microarray were used to assess background signal intensities. Our analyses showed that the distribution of raw signal intensities of all “blank” coordinates on an array approximated a normal distribution with the mean value around 1. Assuming that the raw intensity distributions of these “blank” coordinates (background noises) were the same across all microarrays (under different conditions), we used a  $Z$ -score to set a universal background cutoff for all conditions. Hence, the protein signals were standardized using

$$Z(I) = \frac{I - m}{\sigma}$$

where  $Z$  is  $Z$ -score of each protein coordinate,  $I$  is raw intensity of the coordinate, and  $m$  and  $\sigma$  are mean value and standard deviation, respectively, of “blank” coordinates on the microarray.

### Data Analysis

A mixed-model analysis of variance was used to detect differential phosphorylation for each immobilized protein substrate using Partek software [8]. To assess differential protein phosphorylation for each of the lysate preparations, we first averaged all kinases from a particular experimental group. Substrates on the human kinome chip were assigned to one or more functional groups with a unique ID number based upon GO annotations [9–11]. To assess the statistical significance of phosphorylation differences, we implemented a  $t$  test procedure, which defines phosphorylation as either regulated or not, and employed a Fisher's exact test or hypergeometric distribution analysis. Under the usual assumptions, namely, independence and normality of the error, a  $t$  test offers more power than a test with a dichotomized outcome.

### Clinical Specimens and Cell Culture

Human clinical specimens were obtained from the Johns Hopkins Neurosurgical operating suites. The Johns Hopkins University Institutional Review Board approved all protocols in this study.

The tet-on PTENwt-inducible U87 cell line was a kind gift from Dr. Maria Georgescu (MD Anderson Cancer Center) and cultured as previously described [6,12]. The tetracycline-inducible PTENwt-expressing cell line was developed using a retroviral vector in the PTEN-deficient U87 glioma cell line. Two retroviral constructs,

pCXn/tetracycline repressor (TR2) and pCXbR(TO)-PTEN, were simultaneously introduced to U87 glioma cells by infection. The pCXn/TR2 construct encodes TR of the tetracycline operon that is found in the second construct. The second pCXbR(TO)-PTEN construct contains the inducible promoter that controls transcription of wild-type PTEN. When tetracycline, or its derivative doxycycline, is present, the repressor is inhibited and catalytically active PTEN is expressed. When tetracycline, or its derivative doxycycline, is absent, the repressor prevents PTEN expression from the second retroviral construct.

### Whole Cell Lysate Preparation

Total protein was extracted from glioma xenografts and cells using radioimmunoprecipitation assay buffer (1% Igepal, 0.5% sodium deoxycholate, and 0.05% SDS in PBS) containing fresh  $1 \times$  protease and  $1 \times$  phosphatase inhibitors (Calbiochem) at  $4^{\circ}\text{C}$ . Tissue extracts were sonicated on ice and centrifuged at 5000 rpm at  $4^{\circ}\text{C}$  for 5 minutes. Supernatants were assayed for protein concentrations by Coomassie protein assay (Pierce) according to the manufacturer's recommendations.

### Immunoblot analysis

Aliquots of 40 or 60  $\mu\text{g}$  of total protein were combined with Laemmli loading buffer containing  $\beta$ -mercaptoethanol and subjected to SDS polyacrylamide gel electrophoresis according to the method of Towbin et al. with some modifications [13,14]. For immunoblot analyses, proteins were electrophoretically transferred to nitrocellulose with a semidry transfer apparatus (GE Healthcare) at 50 mA for 60 minutes. Membranes were incubated for 1 hour in Odyssey Licor Blocking Buffer at room temperature and then overnight with primary antibodies at  $4^{\circ}\text{C}$  in 5% BSA in TBS/T. Membranes were then washed  $3 \times$  with TBS/T, incubated with secondary antibody at 1:10,000 for 1 hour in TBS/T, and washed  $3 \times$  with TBS/T, followed by washing  $2 \times$  with TBS. Proteins were detected and quantified using the Odyssey Infrared Imager (LI-COR Biosciences).

### Cell Viability Assay

Cell viability was measured by 3-(4,5-dimethylthiazol-2-yl)-2,5-diphenyl tetrazolium bromide (MTT) assay as previously reported [13]. Cells were plated at 50,000 cells/well in 24-well tissue culture plates and cultured for 24 hours before treatment with specified reagents. Twenty-four to 72 hours after treatment, MTT was added to each well at a final concentration of 150  $\mu\text{g}/\text{ml}$ , and the cells were incubated for 2 hours at  $37^{\circ}\text{C}$ . The medium was then removed, and the cell layer was dissolved with dimethyl sulfoxide. The formazan reaction product was quantified spectrophotometrically at 570 nm using a Spectra MAX 340pc plate reader (Molecular Devices, Sunnyvale, CA). Results are expressed as the percentage of absorbance measured in control cultures after subtracting the background absorbance from all values.

### Tumor Xenografts

Glioma xenografts were generated as previously described [15]. Female 6- to 8-week-old mice (National Cancer Institute, Frederick, MD) were anesthetized by intraperitoneal injection of ketamine (100 mg/kg) and xylazine (5 mg/kg). For subcutaneous xenografts, Nu/nu mice received  $4 \times 10^6$  cells in 0.05 ml of plain media subcutaneously in the dorsal flank. When tumors reached  $\sim 200 \text{ mm}^3$ , the mice were randomly divided into groups ( $n = 5$  per group) and received the indicated doses of

either 5% sucrose or 5% sucrose + 2  $\mu\text{g}/\text{ml}$  of doxycycline in the drinking water as previously described [6]. Tumor volumes were estimated by measuring two dimensions [length ( $a$ ) and width ( $b$ )] and calculating volume as  $V = ab^2/2$  [16,17]. At the end of each experiment, tumors were excised and frozen in liquid nitrogen, and protein was extracted for immunoblot analysis.

The Johns Hopkins University Institutional Animal Care and Use Committee approved all animal protocols used in this study. All experiments were performed in accordance with relevant guidelines and regulations.

Supplementary data to this article can be found online at <http://dx.doi.org/10.1016/j.tranon.2016.02.001>.

### Acknowledgements

We thank Drs. H.-S. Rho and J.-S. Jeong for technical assistance for microarray construction. This work is supported in part by the National Institutes of Health (RO1 CA129192 and RO1 NS43987 to J.L.) and the United Negro College Fund/Merck Science Initiative, Neurosurgery Research and Education Foundation, and Burroughs Wellcome Fund to C. R. G.

The authors report no competing financial interests.

### References

- Mann M and Jensen ON (2003). Proteomic analysis of post-translational modifications. *Nat Biotechnol* **21**, 255–261.
- Newman RH, Hu J, Rho HS, Xie Z, Woodard C, Neiswinger J, Cooper C, Shirley M, Clark HM, and Hu S, et al (2013). Construction of human activity-based phosphorylation networks. *Mol Syst Biol* **9**, 655.
- Woodard CL, Goodwin CR, Wan J, Xia S, Newman R, Hu J, Zhang J, Hayward SD, Qian J, and Laterra J, et al (2013). Profiling the dynamics of a human phosphorylome reveals new components in HGF/c-Met signaling. *PLoS One* **8**, e72671.
- Ptacek J, Devgan G, Michaud G, Zhu H, Zhu X, Fasolo J, Guo H, Jona G, Breitkreutz A, and Sopko R, et al (2005). Global analysis of protein phosphorylation in yeast. *Nature* **438**, 679–684.
- Bellacosa A, Kumar CC, Di Cristofano A, and Testa JR (2005). Activation of AKT kinases in cancer: implications for therapeutic targeting. *Adv Cancer Res* **94**, 29–86.
- Goodwin CR, Lal B, Ho S, Woodard CL, Zhou X, Taeger A, Xia S, and Laterra J (2011). PTEN reconstitution alters glioma responses to c-Met pathway inhibition. *Anti-Cancer Drugs* **22**, 905–912.
- Zhu H, Bilgin M, Bangham R, Hall D, Casamayor A, Bertone P, Lan N, Jansen R, Bidlingmaier S, and Houfek T, et al (2001). Global analysis of protein activities using proteome chips. *Science* **293**, 2101–2105.
- Partek Inc. (2014). <http://www.partek.com>; 2014.
- Ashburner M, Ball CA, Blake JA, Botstein D, Butler H, Cherry JM, Davis AP, Dolinski K, Dwight SS, and Eppig JT, et al (2000). Gene ontology: tool for the unification of biology. The Gene Ontology Consortium. *Nat Genet* **25**, 25–29.
- Eppig J T, Hill D P, Ni L, Ringwald M, Balakrishnan R, Cherry J M, Christie K R, Costanzo M C, Dwight S S, and Engel S, et al (2004). The Gene Ontology (GO) database and informatics resource. *Nucleic Acids Res* **32**, D258–D261.
- Gene Ontology. <http://www.geneontology.org>; 2014.
- Radu A, Neubauer V, Akagi T, Hanafusa H, and Georgescu MM (2003). PTEN induces cell cycle arrest by decreasing the level and nuclear localization of cyclin D1. *Mol Cell Biol* **23**, 6139–6149.
- Goodwin CR, Lal B, Zhou X, Ho S, Xia S, Taeger A, Murray J, and Laterra J (2010). Cyr61 mediates hepatocyte growth factor-dependent tumor cell growth, migration, and Akt activation. *Cancer Res* **70**, 2932–2941.
- Towbin H, Staehelin T, and Gordon J (1979). Electrophoretic transfer of proteins from polyacrylamide gels to nitrocellulose sheets: procedure and some applications. *Proc Natl Acad Sci U S A* **76**, 4350–4354.
- Lal B, Xia S, Aboumader R, and Laterra J (2005). Targeting the c-Met pathway potentiates glioblastoma responses to gamma-radiation. *Clin Cancer Res* **11**, 4479–4486.
- Lal B, Goodwin CR, Sang Y, Foss CA, Cornet K, Muzamil S, Pomper MG, Kim J, and Laterra J (2009). EGFRvIII and c-Met pathway inhibitors synergize against PTEN-null/EGFRvIII+ glioblastoma xenografts. *Mol Cancer Ther* **8**, 1751–1760.
- Tomayko MM and Reynolds CP (1989). Determination of subcutaneous tumor size in athymic (nude) mice. *Cancer Chemother Pharmacol* **24**, 148–154.